

Design Considerations for Holographic Retinal Projection Display

Christophe Martinez, Fabian Rainouard, Basile Meynard

Photonic Systems Laboratory, Univ. Grenoble Alpes, CEA, LETI, DOPT/SISP/LASP, 38054 Grenoble, France

Keywords: retinal display, augmented reality, near-eye display, diffraction.

ABSTRACT

We present design considerations for the development of a retinal projection display based on the association of a photonic integrated circuit and a pixelated hologram. Unexpected behavior concerning the randomness distribution of the emitting elements in our display is highlighted.

1 INTRODUCTION

Micro-displays are currently key elements of near-to-eye Augmented Reality (AR) devices. For these applications, the need to overlay a bright digital image with high resolution over the natural scenery observed by the user constrains the design of the display. Main solutions are OLED and LCOS displays [1,2] and more recently, LED displays have emerged as a technological alternative for higher brightness [3]. However, complex optical systems between the micro-display and the eye are required in the AR smart glasses to focus the digital image in the eye of the user. To overcome these integration issues, unconventional solutions are currently investigated such as lens-less retinal projection [4-6].

CEA Leti has recently proposed a concept of retinal projection display based on the use of silicon photonics and holography. As shown in figure 1, a modulated laser array is distributed through a waveguide network at the surface of a glass. The waveguides transport light signals to angle-selective holographic elements, which generate – in a scanning mode – the wave-fronts forming the image on the retina [7].

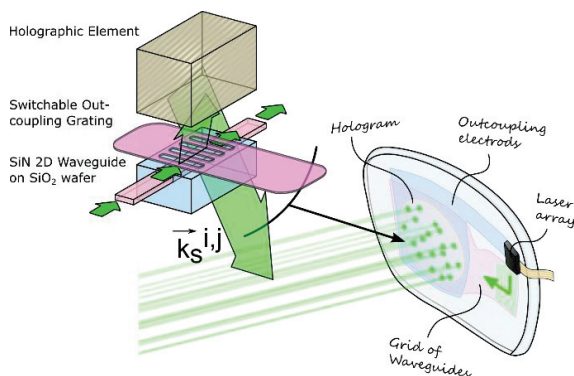


Fig. 1 General principle of the retinal display concept investigated by CEA Leti.

2 SELF-FOCUSING DISPLAY

The retinal imaging process is based on a physical effect called self-focusing. It consists of a multiple interference process that allows a distribution of spherical beams to interfere constructively in a single point, in order to form the Point Spread Function (PSF) of the system. One of the challenges in this display design is the choice of the beam distribution. The beam positions are defined as the Emissive Point Distribution (EPD) of the display.

To validate the self-focusing concept in an image forming configuration, an experimental setup is built [8] using our latest developments in LED micro-displays [3]. Figure 2 presents the experiment: an opaque mask with an aperture distribution that represents an EPD generating a distribution of spherical wave-fronts. These wave-fronts encode specific angular directions so that the interfering process can produce an image in an imaging device that mimics the eye.

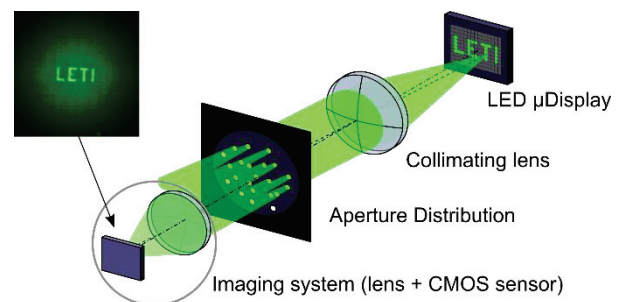


Fig. 2 Set-up used to evaluate the self-focusing effect in a retinal display configuration.

In the experiment, each activated pixel of the display generates a spherical wave-front transformed by the collimating lens into a planar wave-front with a given angular direction. These wave-fronts are diffracted by the Aperture distribution and form the EPDs with the respective angular direction fixed by the activated pixel of the micro-display. Figure 2 shows the wave-fronts associated to a given pixel.

3 RESULTS

We showed in our former analysis that the EPD has to face two contradictory requirements [7]. The first is to avoid periodicity in the distribution to limit the multiple diffraction orders in the image forming process. Second is to address the EPD with a set of waveguides and electrodes in a realistic manner.

Figure 3(a) and 3(b) show a periodic EPD with period Λ . In this case the addressing is simple with linear waveguides and electrodes but the image formed on the sensor is duplicated by the multiple diffraction orders and the image of the micro-display cannot be recognized.

Figure 3(c) and 3(d) show the case of a Quasi Random distribution (QR) where each emissive point is located randomly in the periodic grid. Self-focusing allows image formation on the CMOS sensor to the cost of a large noise contribution that degrades the contrast. This EPD choice corresponds to an ideal imaging case but is difficult to implement for addressing reasons.

Figure 3(e) and 3(f) show a more realistic EPD where the addressing is done by waveguides and electrodes with simple sinusoidal shapes (Cross Random Sinusoidal distribution, CRS). This design introduces a part of randomness in the design but not sufficiently as some ghost images still disturb the imaging performance as shown in figure 3(f).

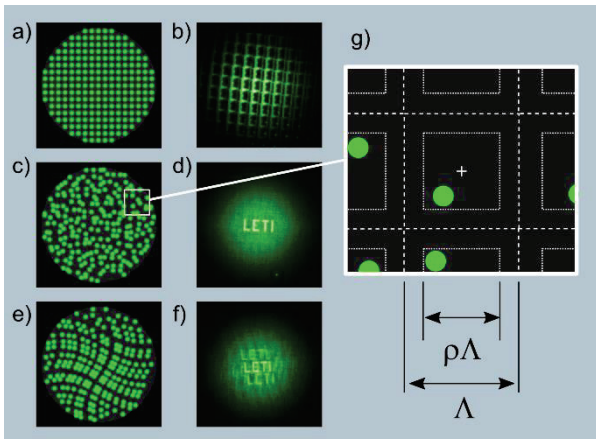


Fig. 3: Results of self-focusing experiments; (a), (c) and (e): EPD in the case of periodic, QR and CRS configurations; (b), (d) and (f) corresponding result of image formation on CMOS sensor; (g) detail of the random configuration.

4 SELF-FOCUSING PERFORMANCE EVALUATION

These measurements and our simulations show that the PSF of the self-focusing device can be characterized by two parameters as shown in figure 4. The first one is the ratio between the peak at the center of the angular domain and the highest secondary peak belonging to the noise contribution. The presence of these ghost peaks is responsible for the ghost images observed in figure 3(f).

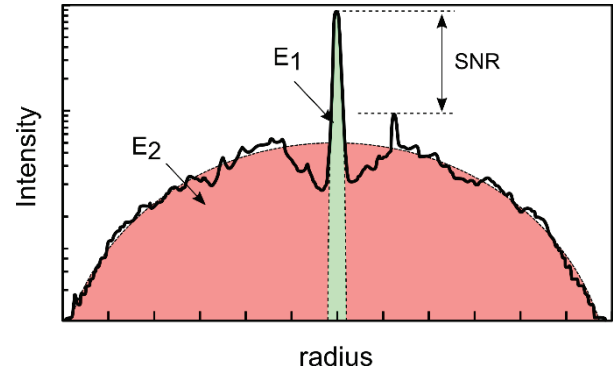


Fig. 4 Parameter SNR and γ characterizing the Point Spread Function resulting from self-focusing.

These peaks/spikes are remains of the peaks caused by the multiple diffraction orders. They indicate that the EPD still has some periodicity. We describe this parameter as a Signal to Noise Ratio given in dB:

$$SNR = 10 \log \left(\frac{I_{peak}}{I_{ghost}} \right)$$

The second parameter is the ratio between the energy E_1 of the central peak and the energy of the whole PSF. We use the letter γ as a reference for this parameter:

$$\gamma = -10 \log \left(\frac{E_1}{E_1 + E_2} \right)$$

5 INFLUENCE OF THE RANDOM CONTRIBUTION

To evaluate the impact of the EPD design on the imaging performance we introduce a randomness coefficient ρ on the QR distribution as shown in figure 3(g). The location (x,y) of each emissive point i,j is given by the equation:

$$\begin{aligned} x_{i,j} &= \Lambda(i + \rho \times rnd) \\ y_{i,j} &= \Lambda(j + \rho \times rnd) \end{aligned}$$

With rnd a random number in the interval $[-0.5;0.5]$.

The periodic case corresponds to $\rho = 0$ (figure 3(a)) and the QR case to $\rho = 1$ (figure 3(c)).

Figure 5 and 6 give the results of our PSF simulations as a function of ρ for different grid periods. The simulation parameters are chosen to be representative of the final retinal design: full eye aperture diameter 4 mm, emissive point diameter $5 \mu\text{m}$ and eye focal length 23 mm [7]. Each simulation is repeated 30 times in order to evaluate the best and worst random draw.

6 ANALYSIS

Our simulations show some unexpected and original considerations for the EPD design. We confirm that the randomness behavior of the EPD has a significant impact on the SNR. However we observe that it exists some design flexibility relative to the ρ coefficient. For a grid period of $400 \mu\text{m}$, the maximum SNR value reaches an asymptote for a random coefficient of about 0.7.

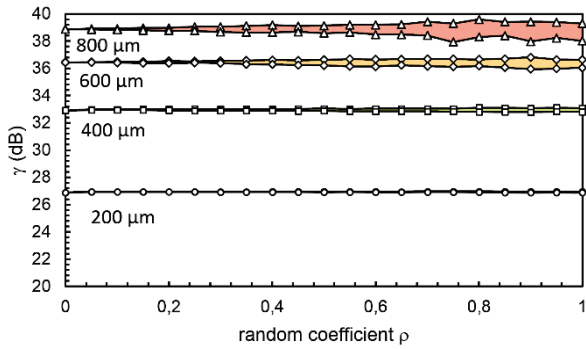


Fig. 5 Peak contrast efficiency γ as a function of the random coefficient ρ for various grid periods (200 μm to 800 μm) for 30 random draws.

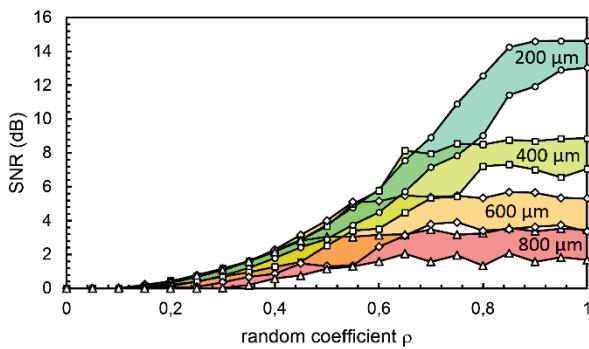


Fig. 6 Peak intensity SNR as a function of the random coefficient ρ for various grid periods (200 μm to 800 μm) for 30 random draws.

For random parameters higher than 0.8 we observe a stabilized maximum/minimum SNR result. This shows that the highest degree of randomness distribution is not necessarily required depending on the distribution grid period.

The results of the γ parameter are more consistent with our expectations. The large noise contribution is directly related to the grid period – i.e. to the number of points in the EPD (referred as the size of the EPD). The randomness factor has little impact on the γ value. For a given grid period, introducing some randomness behavior transform the energy located in the multiple diffraction orders into a large speckle noise contribution with limited change on the central peak energy.

To improve the contrast of the image we need to reduce the grid period for a given pupil aperture, that is we need to increase the size of the EPD. However, as the total number of emissive point is fixed by the pupil aperture, increasing the size of each EPD reduces the total number of EPD – i.e. the number of pixel to be displayed. A compromise has to be found between the image quality in terms of contrast and resolution.

The impact of the SNR on image quality is more difficult to interpret. In our experiment of figure 2 a fixed EPD is common to all the displayed pixel. However in the real

device all the EPD are different and the location of the ghost peaks is not stationary. The ghost images will be averaged on the whole image. This particular aspect of the display concept is currently under study.

As an illustration figure 7 compares the case of a high resolution/low contrast image (figure 7(a)) and the case of a low resolution/high contrast image (figure 7(b)).

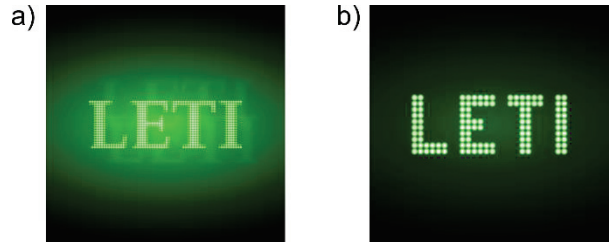


Fig. 7 Example of the word LETI (a) sampled with 64x20 pixels and displayed with bad contrast and (b) sampled with 26x10 pixels and displayed with good contrast.

7 CONCLUSION

This research focuses on the determination of the best EPD design that could fulfill a realistic addressing scheme together with good imaging performances. We have shown that it exists some latency in the random distribution so that a compromise could be found between realistic manufacturing design, good image contrast and resolution.

These complex set of parameters, and their determination for our unconventional retinal display will be described in details during the conference.

REFERENCES

- [1] G. Haas, "Highly Energy Efficient and Compact OLED Microdisplays and their Use in Wearables (invited)," SID-Mid-Europe on Wearable and Projection Displays, Dresden/Germany, (2017)
- [2] R. Likamwa, Z. Wang, A. Carroll, F. X. Lin and L. Zhong, "Draining our glass: An energy and heat characterization of Google Glass." In Proceedings of 5th Asia-Pacific Workshop on Systems, APSYS 2014 Association for Computing Machinery (2014).
- [3] F. Templier, L. Dupré, B. Dupont, A. Daami, B. Aventurier, F. Henry, D. Sarrasin, S. Renet, Berger, F. Olivier, and L. Mathieu, "High-resolution active-matrix 10- μm pixel-pitch GaN LED microdisplays for augmented reality applications," Proc. SPIE 10556, Advances in Display Technologies VIII, 105560I (2018).
- [4] A. Maimone, A. Georgiou, and J. S. Kollin, "Holographic near-eye displays for virtual and

augmented reality," *ACM Trans. Graphics*, 36(4), 85(2017).

- [5] G.-Y. Lee, J.-Y. Hong, S.H. Hwang, S. Moon, H. Kang, S. Jeon, H. Kim, J.-H. Jeong and B. Lee , "Metasurface eyepiece for augmented reality", *Nat. Commun.*9(2018), 4562
- [6] J. Notaros, M. Raval, M. Notaros, and M. R. Watts, "Integrated-Phased-Array-Based Visible-Light Near-Eye Holographic Projector," in *Conference on Lasers and Electro-Optics, OSA Technical Digest (Optical Society of America, 2019)*, paper STu3O.4.
- [7] C. Martinez, V. Krotov, B. Meynard, and D. Fowler, "See-through holographic retinal projection display concept," *Optica* 5(10), 1200-1209 (2018).
- [8] V. Krotov, C. Martinez, and O. Haeberlé, "Experimental validation of self-focusing image formation for retinal projection display," *Opt. Express* 27, 20632-20648 (2019)